Mechanical Systems and Signal Processing 146 (2021) 107052

Contents lists available at ScienceDirect

Mechanical Systems and Signal Processing

journal homepage: www.elsevier.com/locate/ymssp

Effect of boundary conditions in the experimental determination of structural damping

C.A. Geweth *, S.K. Baydoun, F. Saati, K. Sepahvand, S. Marburg

Technical University of Munich – Chair of Vibro-Acoustics of Vehicles and Machines, Germany

ARTICLE INFO

Article history:
Received 30 December 2019
Received in revised form 4 May 2020
Accepted 5 June 2020
Available online 15 July 2020

Keywords:
Structural damping
Experimental modal analysis
Boundary conditions
Acoustic radiation damping

ABSTRACT

Building a digital twin representing the dynamical behaviour of a structure requires knowledge of its material and geometrical properties. While geometry, mass and stiffness can often be characterised quite accurately, at least for homogeneous isotropic materials, the experimental quantification of structural damping is a time consuming endeavour. Furthermore, the chosen experimental set-up subjects the obtained damping values to uncertainties. In this context, the present study takes a closer look at the influence of the boundary conditions on experimentally obtained damping values. A solid plate made out of a commonly used aluminium alloy has been measured repeatedly with different boundary conditions. The plate is excited by an automated impulse hammer and a laser scanning vibrometry has been employed in order to record the structural response at a total of 165 equally distributed points per measurement. Hence, the modal damping values do not only correspond to a segment but to the entire structure. For each boundary condition, the specimen has been measured 20 times consecutively in order to determine the underlying variance. These data point out that experimentally obtained damping values are much more sensitive to the applied boundary conditions than the natural frequencies. Furthermore, it is indicated that the lowest damping values are obtained when suspending the structure at the nodal lines of the corresponding mode. In the second part of this study, the experimentally determined damping values are compared to numerically obtained values for acoustic radiation damping. This comparison suggests that at higher frequencies, the overall damping of the plate is more affected by energy dissipation due to sound radiation than at lower frequencies.

1. Introduction

In recent decades, the demand for more precise and reliable simulation models has increased significantly. It is nowadays good practice in several engineering fields and in some cases required by guidelines or even governmental requirements to do precise prediction of the dynamical behaviour of a structure; as an example, by knowing the density, geometry and stiffness of a component, it is relatively simple, at least for homogeneous models to get a reliable estimate of the natural frequencies [1,2]. Natural frequencies can be calculated quite precisely when the geometry (thickness included) and material parameters are precisely known and the finite element mesh is reliable. However, the variability of eigenfrequencies due to material and geometrical parameters for simple monolithic structures rarely rises above 2% [3]. In this context the need

* Corresponding author.
E-mail address: christian.geweth@tum.de (C.A. Geweth).

https://doi.org/10.1016/j.ymssp.2020.107052
0888-3270/

for reliable damping models and validation techniques is increasing likewise. As an example, results from the work of Ay et al. [4] show that damping estimates can be used for non-destructive damage detection and damage identification. The damping distribution inside a structure can also affect the characteristics of an emitted sound field [5–7]. When it comes to numerical models regarding mechanical damping, several different damping models, e.g. Kelvin-Voigt damping, Biot-Model [8] or Iwan-Model [9], have been developed in the past. Furthermore several researchers have followed the idea to model damping by fractional derivatives of displacement [10–12]. However, the Rayleigh model is still commonly used. This can be derived from the fact that it is one of the few models implemented in commonly used commercial FE-Software [13,14]. Physical mechanisms actively taking part in energy dissipation of a structure are, according to Adhikari [15,16], complicated processes that are not totally understood. Moreover, the energy dissipation is determined by the superposition of several different damping effects. For example, energy dissipation within a material can be caused by microplastic deformations and heat generation induced by deformation. In contact areas like cracks, screwed and clamped joints the damping is caused by friction due to relative motion [17]. Furthermore energy can dissipated through air- and structure-borne-sound into the environment [18,19]. Therefore, simplification and generalization via mathematical tools do not provide detailed physical explanation and are only introduced to obtain a rough estimate of the actual damping behaviour of a structure. The damping models, as Scanlan [20] puts it, are still crutches to give "perhaps acceptable results in limited ranges" and nothing more. As a result, optimal design can be achieved merely through assuming damping values in a numerical model that often have to be updated several times when it comes to experimental validation. Data capture on a structure is in general quite costly and the goal is to decrease the rectification and have less iterations in the design process. A more reliable simulation is necessary to reduce essential safety factors, allow more efficient prediction models, and accurately reflect the form and condition of structures [21].

With the necessity to validate damping inflicted models, it is of utmost importance for damping measurements to be performed on a prototype of the specimen in question. Meaning, for every design iteration, measurements need to be done on the real component and virtual prototyping is hence not doable. Therefore, with every single change in the geometry of the structure, the damping values of the material in use will also change with no clearly predictable pattern. Thus, remeasuring is inevitable for proper validation and a real prediction is nearly impossible. However, when measuring or simulating, potential sources of errors exist. These can be related to equipment calibration or damages, excessive noise, false data interpretation, incorrect sensor location, unsuitable choice of model, parameter uncertainties, lacking details, irreproducible procedures, unfitting boundary condition, and so on [22,23]. For example Carne et al. [24] investigated the influence of the length of elastic strings in the approximation of free-free boundary conditions. To avoid such errors, literature contains examples such as a study by Hentschel *et al.* [25] in which they developed a setup for specimen-specific material damping determination using a vacuum chamber mentioning excitation forces as high as 3 kN. Since vacuum chamber is currently not the most affordable solution to the aforementioned problems, the need for further investigations continues to exist. Amongst the most influential boundary conditions is the mass loading of a shaker and sensors such as accelerometers attached to the specimen. According to Ewins [26], among the boundary conditions, providing a free support is practically unrealisable since holding the structure is a necessity in reality. What we can design as a suspension setup is the closest approximation possible to the free-free condition. Furthermore, the surrounding fluid can affect the obtained values as well as the chosen type of support. Further investigations have been reported by Valentin *et al.* [27], using a nonlinear solution method as an attempt to eliminate the influence of stiffness and damping of the supports on the measurement results.

In this paper, the influence of sensors and the method of excitation is minimised by using a laser scanning vibrometer in combination with an automated impulse hammer. Slightly different versions of approximations of free-free support have been facilitated for the sake of comparison. Furthermore, the damping through emitted sound radiation has been investigated numerically. The structure used in this work is a simple aluminium plate milled out of commonly used alloy. Although aluminium is lightly damped and not a cutting edge material such as composite or similar, it is commonly and widely used across industries. The reason to choose aluminium is its availability in every lab so that the specimen under study is as reproducible as anything can possibly ever be. The current paper is structured as follows: Section 2 introduces the theory behind damping by sound radiation and probability density function correlation and identification. Section 3 describes the specimen and the experimental setup in use, excitation mechanism, data acquisition system, and the post-processing of the data. It is followed by Section 4 in which obtained results are explained, with the focus of the damping induced by the support and damping by sound radiation, separately. Lastly, conclusions are listed in Section 5.

2. Theory

2.1. Damping induced by sound radiation

In addition to material-inherent damping, damping by virtue of sound radiation to the acoustic far-field contributes to the overall energy dissipation of vibrating structures. This effect is commonly denoted as *acoustic radiation damping* and is particularly relevant in lightweight structures. For example, honeycomb sandwich panels can exhibit radiation loss factors of up to $\eta_{\mathrm{rad}} = 0.1$, which clearly exceeds typical values for material inherent damping [28]; see also Fig. 7 in [29]. However, radiation damping is rather small in solid metallic structures, and hence, it is often needless to specifically quantify its extent. The common practice of indicating an overall loss factor that includes all dissipative phenomena is sufficient for

the vibration analysis of these kinds of structures. The aluminium plate considered in this work also falls into this category and does certainly not exhibit large extents of acoustic radiation damping. In the following, we will nevertheless determine its modal radiation loss factors in order to distinguish them from material inherent damping values. Thereby, the effect of radiation damping can be ruled out and the influence of boundary conditions can be studied in an isolated manner.

Experimental procedures to address this issue would require measurements in a vacuum chamber and hence, are associated with an extremely high effort. Furthermore, analytical expressions for radiation damping of unbaffled plates require empirical correction factors [30], and thus are not satisfactory for our purposes. However, recent advances in simulation methods for vibroacoustic problems and nonlinear eigensolvers enable us to numerically determine modal radiation loss factors. These factors will be related to experimentally determined damping values.

In this work, we will follow the numerical procedure as outlined in a previous work of the authors [31]. The vibrational behaviour of the plate is modelled using fully coupled finite and boundary element discretisations. The underlying eigenvalue problem is nonlinear due to the implicit frequency dependency of the boundary element matrices. It is addressed by a contour integral method [32]. The modal radiation loss factors of the individual modes are deduced from the complex eigenvalues. They are inherent properties of the plate and independent of the excitation.

2.2. PDF identification and correlation

The identified damping coefficients for each specimen and each mounting point is assumed to be an uncertain parameter having the probability density function (PDF) of $f(x)$. Conservative PDF identification methods, e.g. Maximum Likelihood Estimator (MLE), enable us to reduce the PDF identification to estimating the parameters of a predefined PDF from available data. Such methods are, however, deductive and converging to a unique PDF is very difficult. For that reason, we employ the Pearson system of the PDF identification. The major advantage is that the identification process only depends on the third and fourth statistical normalised central moments, skewness and kurtosis, respectively. Here, a general form of the Pearson model is used as follows [33,34]

$$\frac{df}{dx} = \frac{x - a_0}{b_0 + b_1 x + b_2 x^2} \tag{1}$$

in which a_0 and b_i are constants and calculated from the third and fourth central statistical moments of the data. Depending on the roots of quadratic function $D = 4b_0b_2 - b_1^2$ and the value of b_2, the solution of the differential equation in Eq. (1) yields to various PDF types, cf. [33] for more details. The normalized central statistical moment, μ_k, of the data with N samples, having the standard deviation of σ are calculated as

$$\mu_k = \frac{1}{N}\sum_{i=1}^{N} \frac{[\hat{x}_i - \mathbb{E}(x)]^k}{\sigma^k}, \qquad k = 3, 4. \tag{2}$$

Here, $\mathbb{E}(x)$ denotes the expected value of the data. Since the estimation of moments is unique, the Pearson system provides a unique PDF for each uncertain parameter.

To detect the strength of dependency and the level of variability in the measured damping coefficients, a correlation analysis is performed. A high correlation means that two or more damping coefficients for various mounting positions have a strong relationship with each other, while a weak correlation shows the variability of the coefficients from each other. This is typically represented by the correlation coefficient $\rho(X_i, X_j)$ between the identified damping at two positions i and j, given by [35]

$$\rho(X_i, X_j) = \frac{\mathbb{E}\{[X_i - \mathbb{E}(X_i)][X_j - \mathbb{E}(X_j)]\}}{\sqrt{\mathbb{E}\left[(X_i - \mathbb{E}(X_i))^2\right]\mathbb{E}\left[(X_j - \mathbb{E}(X_j))^2\right]}}. \tag{3}$$

This gives a value for ρ between -1 and $+1$. While values $\rho \in [-0.3, 0.3]$ show a weak correlation, $|\rho| \geqslant 0.8$ is interpreted as strong correlation.

3. Experiments

It has been the aim of the conducted experiment to obtain damping values for the same specimen under different approximations of the free-free boundary condition. These damping values should be reliable and of statistical significance. Therefore, three different measurement series consisting of 20 single measurements each, were performed with identical settings. Details are described in this section.

3.1. Specimen and experimental setup

A rectangular aluminium (alloy: EN AW 5083 [AlMg4,5Mn07]) plate with the dimensions of 355 mm $\times$ 255 mm $\times$ 13 mm has been used as specimen for the conducted experiments. The total mass of the plate is determined as $m = 3025$ g. A total of

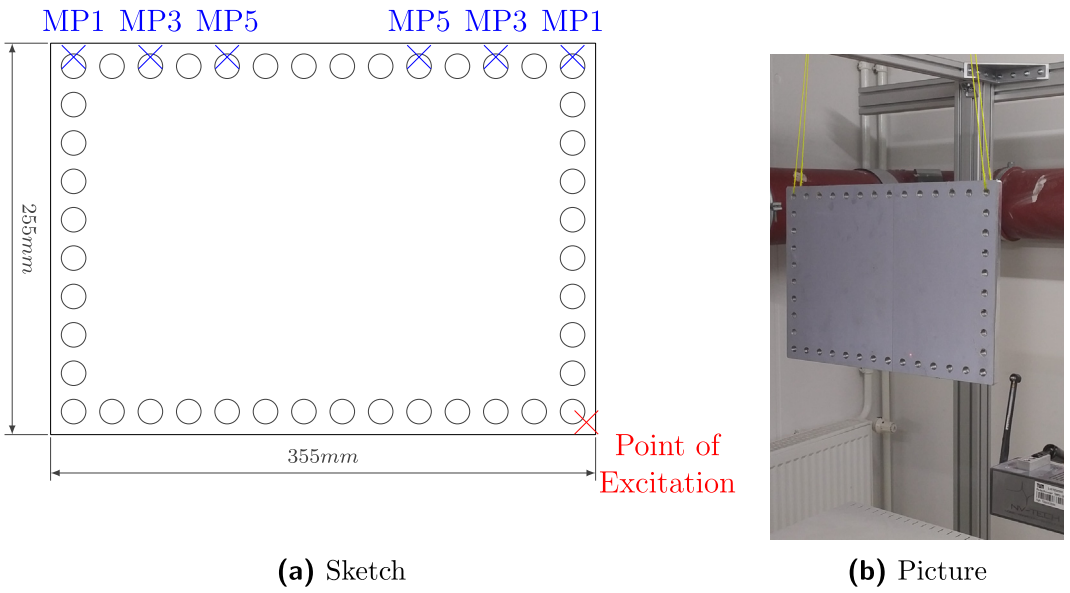

(a) Sketch **(b)** Picture

Fig. 1. Setup.

44 M10 threaded holes are equidistantly positioned around the edges of the plate. These holes are equally distributed so that 25 mm distance remains between consecutive holes. The shortest distance from the center of the holes to the nearest edge of the plate is 12.5 mm. Some of them were utilised as mounting point in the experiments. For that purpose, the strings with a diameter of $\varnothing = 1.5$ mm and a length of $l_{Strings} = 28$ cm were attached to two threaded holes in each measurement series. In Fig. 1a, the holes which were used are marked with a blue cross. In the first measurement series, the two outer holes, labelled with 'MP1' were used. Preliminary testing and simulations suggest that at this point, most of the first ten modes have their highest amplitude. Furthermore, they suggest that several modes have a nodal line at or close to the third hole counting from the corners. Hence, the specimen was suspended in the holes that are labelled with 'MP3' for the second measurement series. For the third measurement series, the strings were attached in fifth holes from the corners or 'MP5'. For each mounting position, the plate has been measured 20 times.

3.2. Excitation and data acquisition

In all measurements, the point of excitation was, as indicated by a red cross in Fig. 1a, located in the lower right corner of the plate. As shown in Fig. 1b, an automated impulse hammer of the type SAM1 built by NV-Tech-Design GmbH [36,37] has been utilised for this purpose. This device was chosen in order to avoid adding mass or damping caused by the method of excitation. For the same reasons, a PSV500 laser scanning vibrometer [26] manufactured by Polytec GmbH was used to record the structural response. On the plate's surface, a total of 165 uniformly distributed measurement points were defined and measured consecutively. For each single point in each measurement, the structure was excited three times and all three recorded signals were averaged and saved to the local drive. The waiting period between the two was set to several minutes, ensuring that any oscillation of the specimen has decayed on the consecutive hit. As a side effect of this waiting period, the recorded time signal could be set to $t_{record} = 40$ s per hit, without prolonging the experiment. In order to identify the amplitude and shape of the hammer impulse, the time resolution was set to $\Delta t = 4 \cdot 10^{-6}$ s. Since the median duration of the impulse is $t_{Impuls} = 44 \cdot 10^{-6}$ s, eleven samples where taken during the hammer hit.

The vibrometer's software PSV 9.2 was utilised in order to record the signal from the vibrometer and hammer. Although some basic signal processing e.g. windowing and Fast Fourier Transform (FFT), lies within the scope of this program, these options were deliberately turned off and only the unprocessed time data were saved on the hard drive. The recorded time data were further processed during the post-processing.

3.3. Post-processing

The non-windowed time data were imported into MATLAB® 2018b [38] and processed further. Here, a force window was put around the impulse. No window function was applied to the vibrometer signal. Subsequently, the time data were transferred into the frequency domain and the frequency response functions are calculated. Since the high sampling rate during the measurement was solely chosen in order to identify the shape, duration and amplitude of the impulse, all frequency data were cut off above the thirteens mode at $f_{max} = 3600$ Hz. The recorded length of the time signal results in a frequency

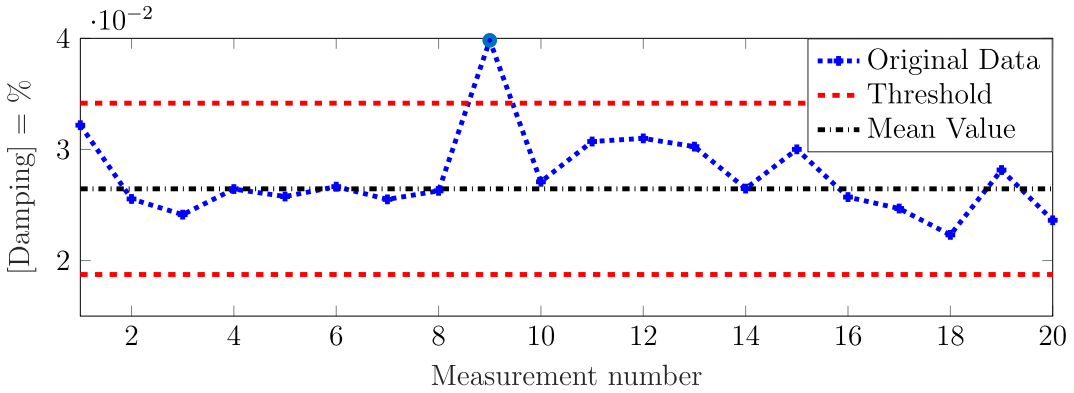

Fig. 2. Outliers mode 2 MP1 – damping values.

resolution of $\Delta f = 0.025$ Hz, allowing a clear identification of the resonance peaks. The obtained FRFs were exported using ME'SCOPE® v17.0.11.24 [39]. By utilising the Z-Polynominal method, an extension of the Rational Fraction Orthogonal Polynomial method, thirteen modes were identified. For each of these modes of each measurement, the natural frequency, the modal damping, and the associated mode shape were exported into MATLAB® for further processing. It should be pointed out that all damping values in this paper refer to the damping ratio, i.e. percent of critical damping. Here, outlier data were removed from the original data set based on a $\pm 3\sigma$ range (see for instance Fig. 2 for mode number 2 'MP1') and the probability density functions are identified.

4. Results

From all obtained modes, a total of four are selected to illustrate the observed influence of the mounting position. Table 1 lists the average of experimentally determined natural frequencies f_{EF} and modal damping values ξ. The arithmetic average is based on all 60 measurements.

The corresponding mode shapes are displayed in Fig. 3. In all four Figures, the plate is orientated as in Fig. 1a. The point of excitation is marked with a red cross while the mounting positions are marked with a dot of blue colour.

4.1. Damping induced by support

The obtained damping results were grouped by their mounting position and the probability density functions were calculated for each mode and mounting position. For the above mentioned modes 2,3,6 and 7, the PDFs are plotted in Fig. 4. The obtained modal damping values differ noticeably between the three mounting positions as well as when repeated for the same mounting position. For all four modes, the lowest damping values were obtained at mounting position 'MP3'. The PDFs of 'MP3' hardly overlap with the damping values obtained at the other two mounting positions.

For the second mode as can be seen in Fig. 4a, an overlap of the PDFs for the damping values obtained for 'MP1' and 'MP5' can be observed. For modes 6 and 7, the overlap between the PDFs of all three mounting is less than for mode 2. One possible

Table 1
Natural frequencies and damping values.

Mode	2	3	6	7
$[f_{EF}] = \mathbf{Hz}$	545.96	1075	1600.11	2004.29
$[\xi] = \%$	0.025	0.0322	0.1024	0.0797

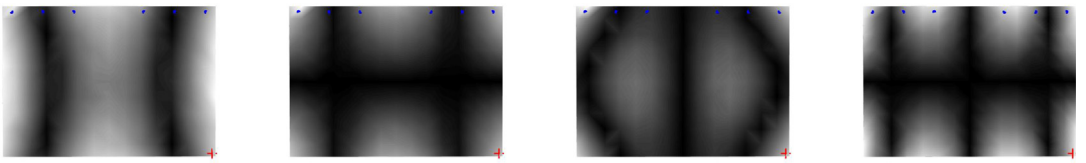

(a) Mode 2 **(b)** Mode 3 **(c)** Mode 6 **(d)** Mode 7

Fig. 3. Mode Shapes.

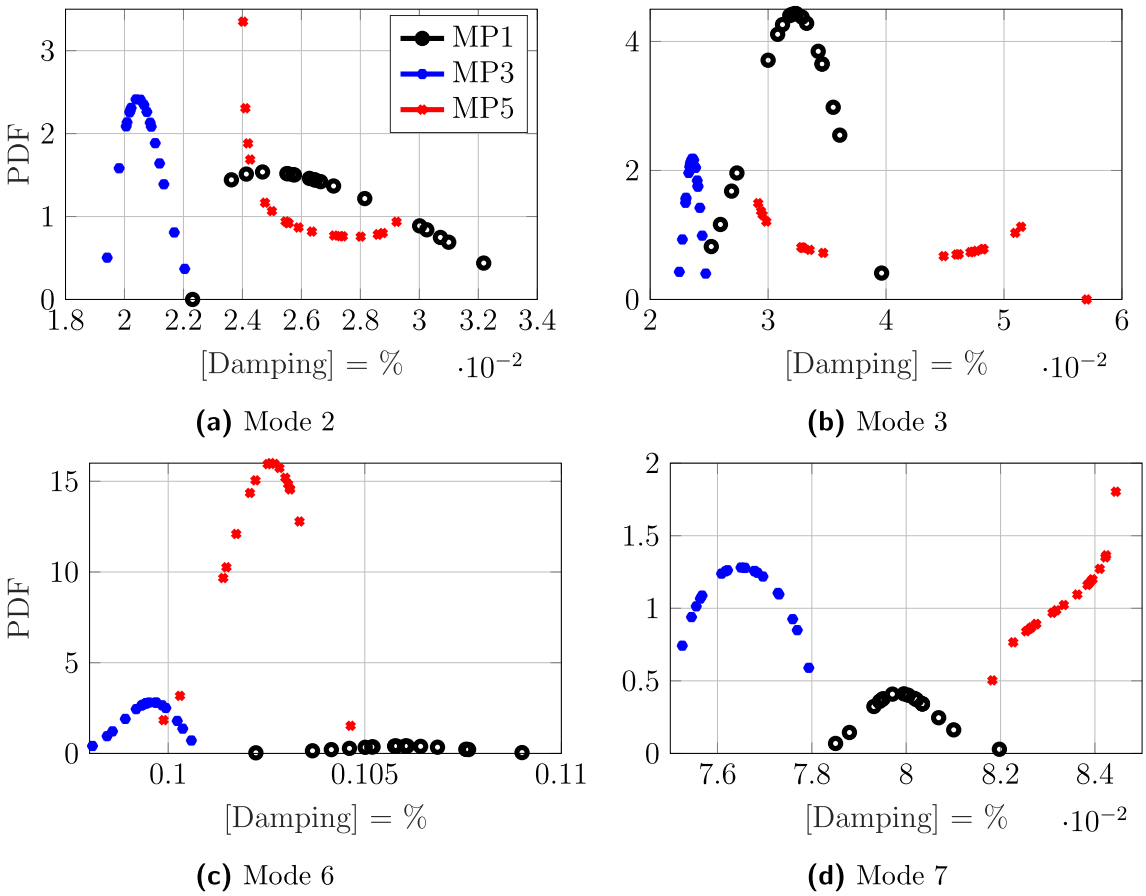

Fig. 4. Probability density function – Damping.

explanation for this observation can be found in the amplitude of the respective mode shape at the mounting point. While for mode 2 the amplitude of the displacement at 'MP1' and 'MP5' is of similar scale and 'MP3' nearly at a nodal line, for mode 6, the amplitude at 'MP1' is larger than at 'MP5' where the amplitude is larger than at 'MP3'. Likewise for mode 7, the amplitude at 'MP5' are larger than at 'MP1' and 'MP3'.

Although the observed difference in damping values are relatively small in absolute numbers, the deviation between the mounting positions in percentage could be considered quite large. As an example, the mean damping value for mode 2 at 'MP1' with a value of $\xi_{2MP1} = 0.02762\%$ is about 31% higher than at 'MP3' ($\xi_{2MP3} = 0.02106\%$). For mode 3, a deviation of 74% between the mean damping values of 'MP5' and 'MP3' can be observed. At this point it should be mentioned, that the obtained natural frequencies are hardly effected by the different type of supports. For instance the difference between the highest and lowest natural frequency obtained for mode 7 is $\Delta f = 1.4$ Hz.

In order to identify dependencies between the different mounting positions, the correlation coefficients are calculated according to Eq. 3 and listed in Table 2. Since the obtained coefficients have quite low values, it can be stated that there is no or only little correlation between damping values obtained at different mounting positions.

Table 2
Correlation coefficients between different damping values.

Mode	2	3	6	7
$\boldsymbol{\rho}(\xi_{\text{MP1}}, \xi_{\text{MP3}})$	0.154	−0.463	0.463	−0.406
$\boldsymbol{\rho}(\xi_{\text{MP1}}, \xi_{\text{MP5}})$	0.087	−0.044	−0.316	0.361
$\boldsymbol{\rho}(\xi_{\text{MP3}}, \xi_{\text{MP5}})$	−0.025	0.565	−0.54	−0.509

Table 3
Measured damping, damping due to and without sound radiation.

Mode	2	3	6	7
$[\xi_{\mathbf{measured}}] = \%$	0.0211	0.0236	0.0992	0.0765
$[\xi_{\mathbf{air}}] = \%$	0.0092	0.0137	0.0951	0.0965
$[\xi_{\mathbf{vacuo}}] = \%$	0.0118	0.0099	0.0041	−0.0199

4.2. Damping due to sound radiation

The numerically determined damping caused by sound radiation is compared to the experimentally obtained damping values [31]. Assuming that the mounting position at which the lowest damping value was obtained is the one influenced the least by the suspension, that one is compared in this Section to the damping induced by sound radiation. Since the reason for the deviation between measurements with the same mounting position has not been clarified, the arithmetic average of the damping values for that particular mounting position was selected as a reference value. In Table 3, this mean damping value is referred to as $\xi_{measured}$. The calculated damping due to sound radiation is referred to as ξ_{Air}. Presuming that the air is effecting the specimen only due to the emission of sound, damping in vacuum ξ_{vacuo} could be determined by subtracting ξ_{Air} form $\xi_{measured}$.

The data in Table 3 show that the radiation due to sound is not negligible for the investigated structure. While for the second and third mode, the damping caused by sound radiation is about half of the measured damping for the sixth, the data suggests that most of the measured damping is caused by sound radiation. For mode 7, the damping without air ξ_{vacuo} seems to be negative. This result is clearly not physically correct and raises the question of other sources of error in the measurement as well as in the simulation. One possible source of error in the experimental setup could be additional excitation from the suspension as well as sound reflection from the laboratory walls. A possible solution to this problem would be to perform the experiments in an anechoic chamber or to include the lab in the numerical simulations.

Additionally, the precision of the numerical solver has to be discussed. The accuracy of each numerically determined eigenpair $(\lambda_i, \mathbf{x}_i)$ can be assessed by the relative backward error

$$\epsilon_{\mathrm{rel},i} = \frac{\|\mathbf{A}(\lambda_i)\mathbf{x}_i\|_2}{\|\mathbf{x}_i\|_2}, \tag{4}$$

where $\mathbf{A}(\cdot)$ denotes the frequency dependent vibroacoustic system matrix. Although the contour integral method yields good accuracy with relative errors $\epsilon_{\mathrm{rel},i}$ of order $\mathcal{O}(10^{-5})$, the actual modal values for radiation damping of the aluminium plate should be understood as rough indication only. This becomes clear when recalling that the modal damping values are given by the ratio of imaginary to real parts of the complex eigenfrequencies. For the modal damping values of the aluminium plate, this ratio is of order $\mathcal{O}(10^{-3})$, which in turn means that the accuracy of the radiation damping values is significantly limited. However, they can still serve as an indication for the extent of radiation damping of each individual mode.

5. Conclusion

The influence of different boundary conditions on the modal damping in an experimental setup has been investigated. Three different versions of an approximation of a free-free boundary condition were realised for that purpose and measured repeatedly. The obtained damping values suggest that a change in the mounting position has a significant effect on the measured damping, although it has hardly any effect on the natural frequencies. A plausible explanation was found in the amplitude of each mode at the mounting position. Hence, it seems to be a necessity to mount a specimen at its nodal lines of investigated mode.

Furthermore, the damping due to sound radiation has been calculated and compared to the measured damping values. At least for this kind of lightly damped materials, the influence of the surrounding fluid on the damping of a specimen seems to have a non-ignorable effect. Although in this study the question of the precision of the numerical solver as well as the influence of the lab has emerged, the chosen procedure to subtract the numerically determined damping by sound radiation from the experimentally determined damping seems to be an effective and cost efficient way of estimating the in vacuo damping of a specimen. Its could be especially true for larger structures since it eliminates the need for a sufficiently sized vacuum chamber and the time needed for its evacuation.

CRediT authorship contribution statement

C.A. Geweth: Conceptualization, Methodology, Investigation, Formal analysis, Data curation, Writing - original draft, Writing - review & editing, Software, Visualization, Validation, Resources, Project administration. **S.K. Baydoun:** Data curation, Writing - original draft, Software, Methodology, Software, Formal analysis, Funding acquisition, Conceptualization. **F. Saati:** Writing - original draft, Writing - review & editing, Resources. **K. Sepahvand:** Supervision, Software, Data curation,

Writing - original draft, Resources, Visualization, Formal analysis, Conceptualization. **S. Marburg:** Supervision, Conceptualization, Funding acquisition, Resources, Project administration.

Declaration of Competing Interest

The authors declare that they have no known competing financial interests or personal relationships that could have appeared to influence the work reported in this paper.

Acknowledgments

The contribution of S. K. Baydoun to this work was supported by the German Research Foundation (DFG) in the context of the priority program 1897 "Calm, Smooth and Smart - Novel Approaches for Influencing Vibrations by Means of Deliberately Introduced Dissipation."

References

[1] M. Friswell, J. Mottershead, Methods using frequency domain data, in: Finite Element Model Updating in Structural Dynamics, Springer, 1995, pp. 228–256.
[2] M. Link, Updating of analytical models—basic procedures and extensions, in: Modal Analysis and Testing, Springer, 1999, pp. 281–304.
[3] P. Langer, K. Sepahvand, C. Guist, J. Bär, A. Peplow, S. Marburg, Matching experimental and three dimensional numerical models for structural vibration problems with uncertainties, J. Sound Vib. 417 (2018) 294–305.
[4] A.M. Ay, S. Khoo, Y. Wang, Probability distribution of decay rate: a statistical time-domain damping parameter for structural damage identification, Struct. Health Monit. 18 (1) (2019) 66–86.
[5] O. Unruh, M. Sinapius, H.P. Monner, Sound radiation properties of complex modes in rectangular plates: a numerical study, Acta Acustica united with Acustica 101 (1) (2015) 62–72.
[6] O. Unruh, Parametric study of sound radiation properties of complex vibration patterns in rectangular plates using an analytical model, Acta Acustica united with Acustica 101 (4) (2015) 701–712.
[7] D. Liu, S. Marburg, C. Geweth, N. Kessissoglou, Non-negative intensity for structures with inhomogeneous damping, J. Theor. Comput. Acoustics 27 (01) (2019) 1850050.
[8] M.A. Biot, Variational principles in irreversible thermodynamics with application to viscoelasticity, Phys. Rev. 97 (6) (1955) 1463.
[9] W.D. Iwan, On a class of models for the yielding behavior of continuous and composite systems, J. Appl. Mech. 34 (1967) 612–617.
[10] L. Gaul, P. Klein, S. Kemple, Damping description involving fractional operators, Mech. Syst. Signal Process. 5 (2) (1991) 81–88.
[11] R.L. Bagley, P.J. Torvik, Fractional calculus-a different approach to the analysis of viscoelastically damped structures, AIAA J. 21 (5) (1983) 741–748.
[12] N. Maia, J. Silva, A. Ribeiro, On a general model for damping, J. Sound Vib. 218 (5) (1998) 749–767.
[13] Dassault Systèmes – Simulia, ABAQUS/CAE 2018 Documentation, 2017.
[14] ANSYS, INC., ANSYS 2019R1 Help, 2019.
[15] S. Adhikari, J. Woodhouse, Identification of damping: Part 1, viscous damping, J. Sound Vib. 243 (1) (2001) 43–61.
[16] S. Adhikari, J. Woodhouse, Identification of damping: Part 2, non-viscous damping, J. Sound Vib. 243 (1) (2001) 63–88.
[17] S. Bograd, P. Reuss, A. Schmidt, L. Gaul, M. Mayer, Modeling the dynamics of mechanical joints, Mech. Syst. Signal Process. 25 (8) (2011) 2801–2826.
[18] VDI-Guideline 3830 Parts 1–5, Damping of materials and members, 2004–2005.
[19] L. Gaul, Tutorial guideline vdi 3830: Damping of materials and members, Topics in Modal Analysis I, vol. 5, Springer, 2012, pp. 25–31.
[20] R. Scanlan, Linear damping models and causality in vibrations, J. Sound Vibr. 13 (1970) 499–503.
[21] L. Bolognini, "An overview of enhanced modal identification, in: Parameter Identification of Materials and Structures, Springer, 2005, pp. 1–15.
[22] P. R. Novak, N. Barbieri, R. Barbieri, Damping identification through use of noncontact sensors, in Sixth International Conference on Vibration Measurements by Laser Techniques: advances and Applications, vol. 5503, pp. 310–319, International Society for Optics and Photonics, 2004.
[23] N. Barbieri, P.R. Novak, R. Barbieri, Experimental identification of damping, Int. J. Solids Struct. 41 (13) (2004) 3585–3594.
[24] T.G. Carne, D.T. Griffith, M.E. Casias, Support conditions for experimental modal analysis, Sound Vibr. 41 (6) (2007) 10–16.
[25] O.P. Hentschel, M. Bonhage, L. Panning-von Scheidt, J. Wallaschek, M. Denk, P.-A. Masserey, Analysis of an experimental setup for structural damping identification, J. Theor. Appl. Mech. 54 (1) (2016) 27–39.
[26] D. J. Ewins, Modal Testing. Wiley, second ed., 2000.
[27] C. Valentin, D. Klerk, D. Rixen, A modal parameter identification method for the elimination of support influences in experimental modal analysis, in: Proceedings of ISMA2008 - International conference on noise and vibration engineering, 2008, pp. 2695–2708.
[28] B.L. Clarkson, K.T. Brown, Acoustic radiation damping, J. Vibr. Acous Stress Reliab. Des. 107 (1985) 357–360.
[29] S.K. Baydoun, M. Voigt, C. Jelich, S. Marburg, A greedy reduced basis scheme for multifrequency solution of structural acoustic systems, Int. J. Numer. Meth. Eng. 121 (2) (2020) 187–200.
[30] C. Oppenheimer, S. Dubowsky, A radiation efficiency for unbaffled plates with experimental validation, J. Sound Vib. 199 (3) (1997) 473–489.
[31] S.K. Baydoun, S. Marburg, Investigation of radiation damping in sandwich structures using finite and boundary element methods and a nonlinear eigensolver, J. Acoust. Soc. Am. 147 (3) (2020) 2020–2034.
[32] S. Yokota, T. Sakurai, A projection method for nonlinear eigenvalue problems using contour integrals, JSIAM Lett. 5 (2013) 41–44.
[33] E.S. Pearson, Some problems arising in approximating to probability distributions using moments, Biometrika 50 (1/2) (1963) 95–112.
[34] K. Sepahvand, S. Marburg, Non-sampling inverse stochastic numerical–experimental identification of random elastic material parameters in composite plates, Mech. Syst. Signal Process. 54–55 (2015) 172–181.
[35] J. Lee Rodgers, W.A. Nicewander, Thirteen ways to look at the correlation coefficient, Am. Stat. 42 (1) (1988) 59–66.
[36] P. Blaschke, T. Mallareddy, D. Alarcón, Application of a scalable automatic modal hammer and a 3d scanning laser doppler vibrometer on turbine blades, in: Proceedings of the 4th VDI conference in vibration analysis and identification, VDI-Berichte, vol. 2259, p. 87, 2016.
[37] P. Blaschke, S. Schneider, R. Kamenzky, D.J. Alarcón, Non-linearity identification of composite materials by scalable impact modal testing, in Sensors and Instrumentation, vol. 5, Springer, 2017, pp. 7–14.
[38] The MathWorks Inc., Natick, Massachusetts, MATLAB Documentation version 9.5.0 (R2018b), 2018.
[39] Vibrant Technology, Inc., Centennial, Colorado, ME'Scope Version 17.0.11.24 Documentation, 2017.